Fluorescence lifetime imaging of human skin and hair

A. Ehlers[1], I. Riemann[1], T. Anhut[1], M. Kaatz, P. Elsner, K. König[1*]

[1]Fraunhofer Institute of Biomedical Technology (IBMT)
Ensheimer Strasse 48, D-66386 St. Ingbert, Germany

[2]Dept. of Dermatology and Allergology
Friedrich Schiller University
Erfurter Strasse 35, D-07743 Jena,Germany

Multiphoton imaging has developed into an important technique for in-vivo research in life sciences. With the laser System DermaInspect (JenLab, Germany) laser radiation from a Ti:Sapphire laser is used to generate multiphoton-absorption deep in the human skin *in vivo*. The resulting autofluorescence radiation arises from endogenous fluorophores such as NAD(P)H, flavines, collagen, elastin, porphyrins und melanin. Second harmonic generation (SHG) was used to detect collagen structures in the dermal layer. Femtosecond laser multiphoton imaging offers the possibility of high-resolution optical tomography of human skin as well as fluorescence lifetime imaging (FLIM) with picosecond time resolution.
In this work a photon detector with ultrashort rise time of less than 30ps was applied to FLIM measurements of human skin and hair with different pigmentation. Fluorescence lifetime images of different human hair types will be discussed.

1. INTRODUCTION

Multiphoton autofluorescence imaging with near-infrared (NIR) femtosecond lasers[1-5] for the diagnosis of skin is an established painless method to examine patients under natural physiological *in vivo* conditions. Photons absorbed via multiphoton excitation can induce autofluorescence based on naturally occurring endogenous fluorescent biomolecules such as flavines, reduced nicotinamide adenine dinucleotide(phosphate) [NAD(P)H], coenzymes, metal-free porphyrins, components of lipofuscin, melanin, elastin and keratin. A further effect is second harmonic generation (SHG) of collagen. *In vivo* analysis of the fluorophores can be carried out by Fluorescence Lifetime Imaging (FLIM) and Confocal Raman Spectroscopy[6]. Three-dimensional (3D) optical imaging of tissue is possible with a spatial resolution of <1µm due to its inherent sectioning properties. JenLab GmbH, Germany, recently launched the first commercial system DermaInspect™ for multiphoton tomography of patients. Different dermatological disorders were examined with this system. Here, the first multiphoton studies of human hairs are presented. Other methods for chemical analysis are, e.g. laser-induced breakdown spectroscopy (LIBS)[7], mass spectrometry[8] and electron microscopy[9] which provide information mainly on chemical composition, but do not yield structural information while being possibe for in vivo investigation. However, all of these methods have in common that preparation of the samples takes time and the sample is destroyed before or during the investigation.
The structure of hairs is described by Zahn[10] and Van Neste[11]: Hair is an skin appendage wich emerges from a follicle, a tubular invagination of the skin. The hair shaft itself is a keratinised structure composed of three layers. The outer layer is called cuticle and is a tile-like protective layer of keratinised cells with a thickness of about 5µm. The bulk of the hair, the cortex, is composed of spindle cells with lengths of about 100µm. The innermost layer is called medulla. Here the cells are larger, less tight connected and partially separated by air spaces. The medulla is present only in thick hairs. Typical average diameters of a human hair are between 55µm and 85µm. The cross-section is elliptical.
Responsible for the coloration of hairs are melanin granules. Of the three different types of melanin, eumelanin, pheomelanin and neuromelanin, only the former two can be found in human hairs. Pheomelanin is predominant in blond and red hairs, whereas eumelanin is a major part in black and brown hairs. The melanin granules are arranged in ellip-

Further author information: (Send correspondence to: Karsten König)
E-Mail: karsten.koenig@ibmt.fraunhofer.de, Telephone: +49(0) 6894 – 980 150

Multiphoton Microscopy in the Biomedical Sciences VI, edited by Ammasi Periasamy, Peter T. C. So,
Proc. of SPIE Vol. 6089, 60890N, (2006) · 1605-7422/06/$15 · doi: 10.1117/12.645714

soid-like melanin granules with a size of about 0.8-1.0µm x 0.3-0.4µm, the long axis is parallel aligned to the cortex fibers.

2. MATERIALS AND METHODS

2.1 Laser scanning system

In this work, the multiphoton tomograph DermaInspect™ was used. A detailed description of the system is published by König et al.[4] Its major modules consist of (see Fig. 1):

A compact, solid state, turnkey, mode-locked titanium:sapphire laser:
Chameleon (Coherent Inc., USA) with tuneable wavelength between 720 nm and 930 nm, a maximum laser output of about 1 W, 150 fs pulse width and 90 MHz repetition rate
A scanning module, including shutter and motorized beam attenuator; a fast x,y-galvoscanner; a piezodriven mount for focusing objective; a photomultiplier tube (PMT, H5773P, Hamamatsu) with short rise time for intensity imaging and a Becker&Hickl PMH100 with transient spread time of 150ps for lifetime measurements and a module with a 0.17 µm thick glass window for *in vivo* measurements. For *in vivo* imaging of skin a 40x objective with NA 1.3 (oil) is used.
In addition, an R3809U-50 MCP (Hamamatsu) was employed.
A control module with power supplies; image-processing hardware and software.

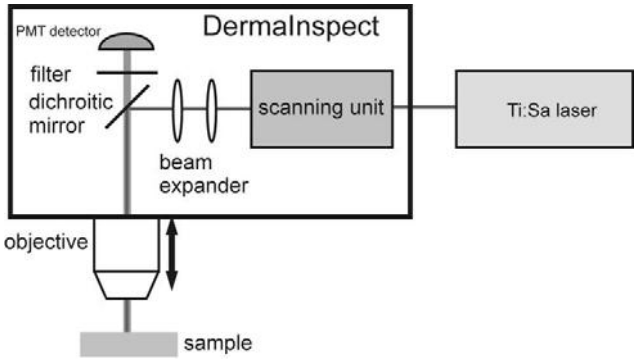

Fig. 1: General experimental setup. The laser passes a scanning unit, beam expander and is deflected into a microscope objective by a dichroic mirror. The focusing optics can be adjusted along the optical axis (z-direction) by piezo controllers.

Multiphoton tomography images were obtained with scan times of 1-25s. For high signal-to-noise ratios 25s for images with 512 x 512pixel were used.
The system was further equipped with a BG39 filter and a 700nm-shortpass filter (Fig.1) to prevent scattered or reflected laser light to enter the detector.
Fluorescence lifetime imaging was performed by time-resolved single-photon counting (TCSPC)[4,12]. Single fluorescence photons have been counted with a fast PMT with ultrashort time spread of 24ps (Hamamatsu R3809U-50 MCP). The PMT signal was synchronized with the lateral beam position on the sample and recorded with an TCSPC-module (SPC-830, Becker&Hickl, Germany). That way, images with 128x128px were obtained with a complete fluorescent lifetime curve for every pixel in the image. FLIM images were also analyzed via the distribution of the different lifetimes over the image. To get a better signal to noise ratio and to prevent photobleaching and damage to the sample, a single FLIM image was obtained by accumulating 10s-scans twenty times.
For imaging a excitation wavelength of 740nm was chosen, the mean laser Power was up to 35mW in deep skin tissue. Hairs were imaged with a mena power of 5mW.

The curve fitting as well as the calculation of histograms was performed with the Becker&Hickl Software package. A bi-exponential fit to the measured fluorescence lifetimes was used. The recorded intensity *I(t)* measured by the detector is a convolution of the fluorescence decay *F(t)* with the instrumental response function *R(t)*:

$$I(t) = F(t) \otimes R(t)$$

with

$$F(t) = A_1 e^{-t/\tau_1} + A_2 e^{-t/\tau_2}$$

For further evaluation of the fluorescence decay characteristics, the lifetime distribution was obtained. Since the total number of pixels of a FLIM image is dependent on the size of the sample visible in the scan, the histogram curves of the lifetime distribution were normalized.

2.2 Sample preparation

Hair samples were freshly cut from human volunteers, rinsed with water, placed on a microscope slide with water and sealed under a coverslip. The samples were imaged immediately after preparation.

For comparative studies of the melanin type found in human hairs, samples of artificial melanin (DOPA-melanin, Sigma-Aldrich) in distilled water (0.1mg/ml) were prepared.

Collagen type 1 (Sigma-Aldrich) was used to determine the TCSPC Instrument Response Function (IRF).

3. RESULTS AND DISCUSSION

3.1 *In vivo* imaging of human skin

An image of the stratum spinosum of *in vivo* human skin is shown in Fig. 2. The scan was obtained with an exposure time of 13.4sec per frame using the PMH100. The lifetime decay curve is shown for a typical pixel; the fast component is determined to be 0.4ns and the slow component to be 2.4ns.

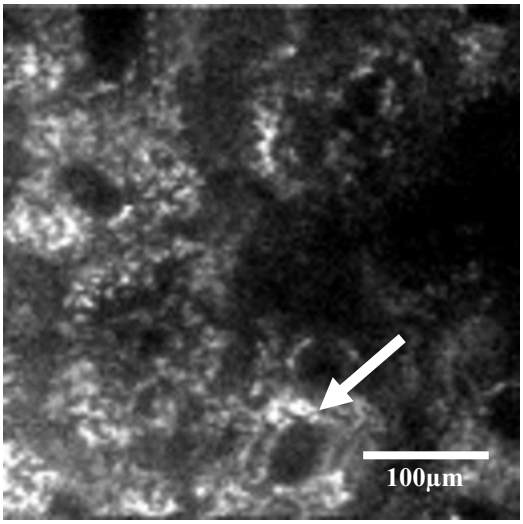

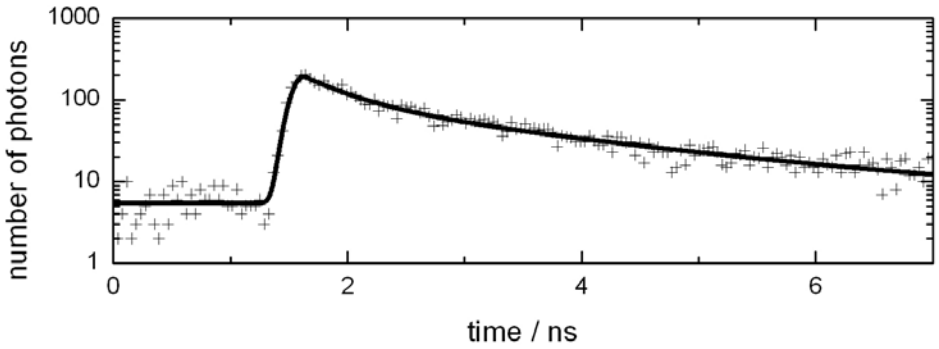

Figure 2: FLIM of in vivo human skin taken with the DermaInspect and a PMH100 detector with time resolution of 150ps. The decay curve of the image point indicated by the arrow shows a fast component of 0.4ns.

In orderc to resolve the fast component, a faster detector system (R3809U-50 MCP) was employed.
At first the instrument response function (IRF) was determined with the fast PMT. As described in Ulrich et al.[12] collagen type 1 was used to generate an SHG signal using a laser wavelength of 840nm (Fig. 3). The FWHM of the time resolution was determined to be 24ps.

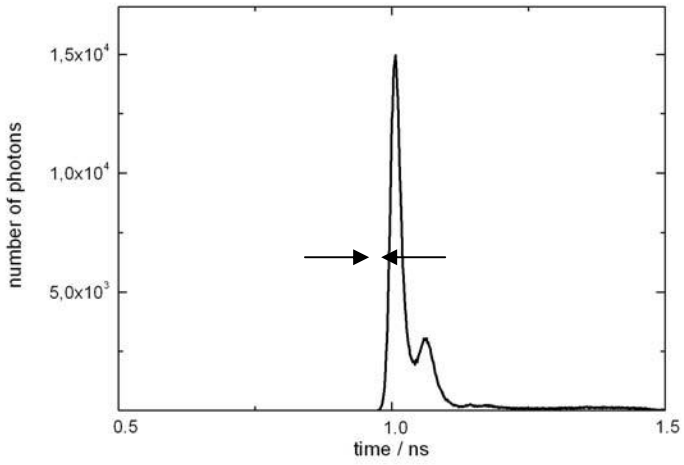

Figure 3: Instrument response function of the fluorescence lifetime detection system with the MCP. The FWHM of the IRF was measured as SHG signal from artificial collagen type I.

In Fig 4 FLIM images of in vivo human skin are shown. Fig 4a) shows the stratum corneum, 4b) the stratum spinosum 4c) stratum basale and 4d) an image of the upper dermis.

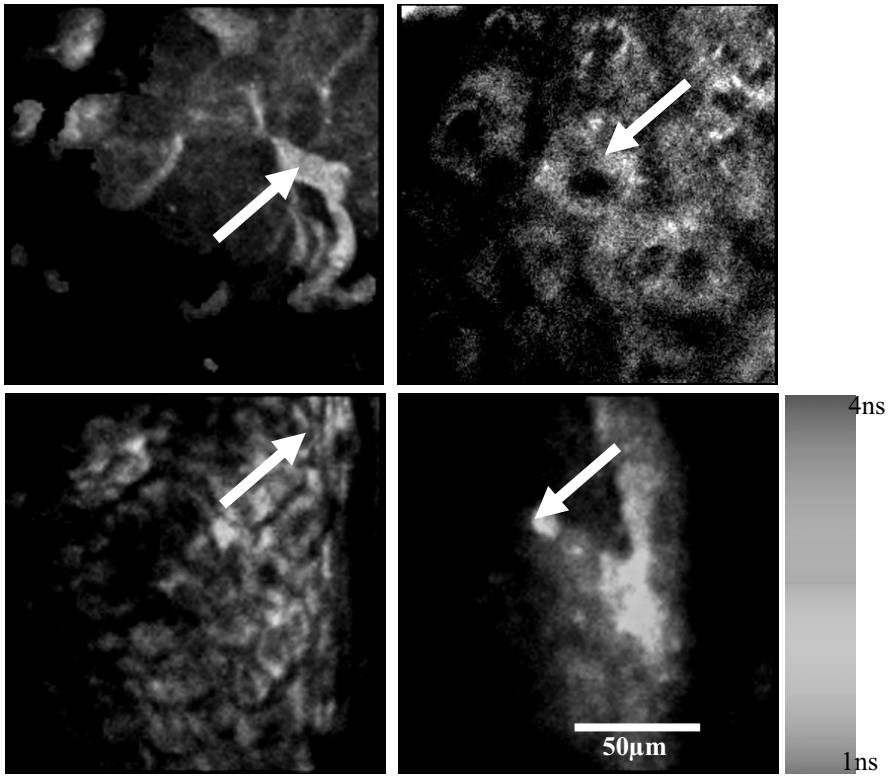

Figure 4: FLIM images of human skin: a) stratum corneum, b) stratum spinosum c) stratum basale d) upper part of dermis. The arrows indicate the lifetime decay curves shown in Fig. 5.

Fig. 5 shows the respective lifetime decay curves at the places as indicated by arrows.

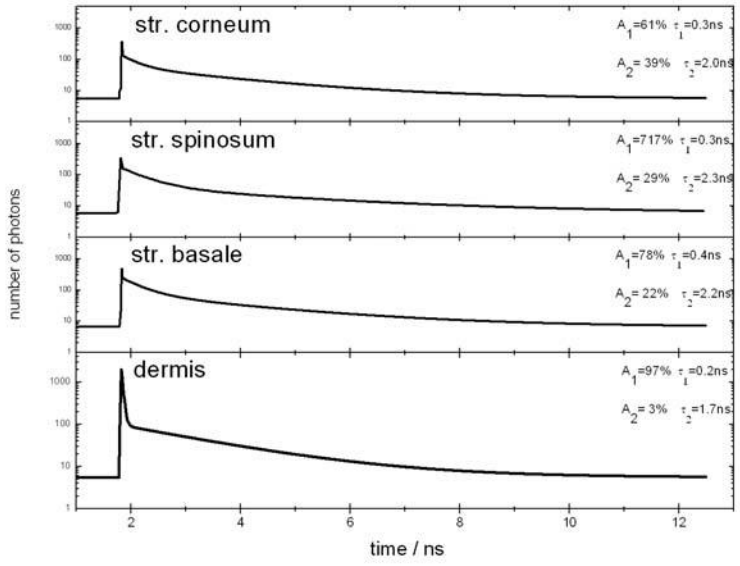

Figure 5: Fluorescence lifetime decay curves of the points indicated by arrows in Fig. 4.

A typical fast decay time of 0.2-0.4 ns was detected. The fast component is more predominant in the dermal layer than in the epidermal layers. In order to make sure that the fast component is due to SHG from the collagen, the influence of scattered light was investigated. Orange fluorescent microbeads (Molecular Probes) with diameter of 170nm were applied on human skin. Fig. 6 a) shows a FLIM image of human stratum corneum with microbeads. The decay times for a microbead and for the stratum corneum were compared to each other (Fig. 6b). In part trapping effects were observed which resulted in non-spherical images of the beads.

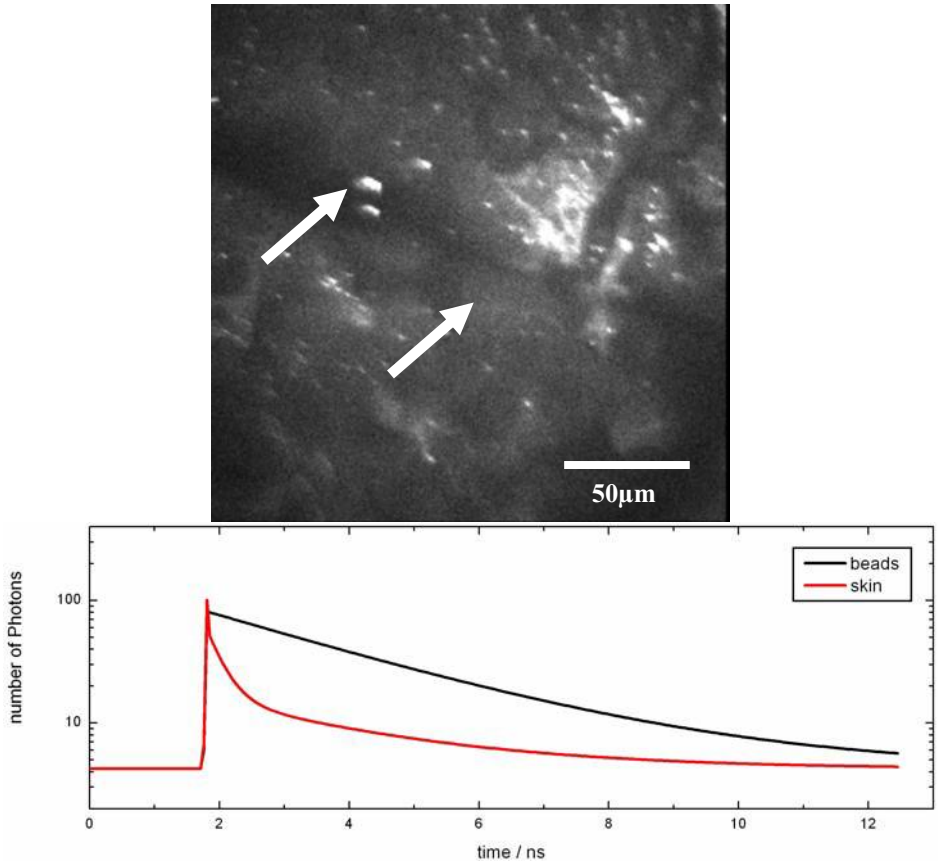

Figure 6: a) Image of orange fluorescent beads on the skin surface (stratum corneum). b) Lifetime decay curves of a microbead and the skin surface, at a locationindicated by arrows in a).

The microbeads exhibited a purely mono-exponential decay curve of 2.6 ns, whereas the decay of the stratum corneum is best fitted with a bi-exponential decay. If scattered light would be able to enter the detector, the decay curve of the microbeads should show a fast component as well. Therefore scattering effects can be excluded and the fast component appears to be an intrinsic property of the human skin.
In Fig. 7 the distribution of the two decay times $_1$ and $_2$ are shown for the different skin regions.

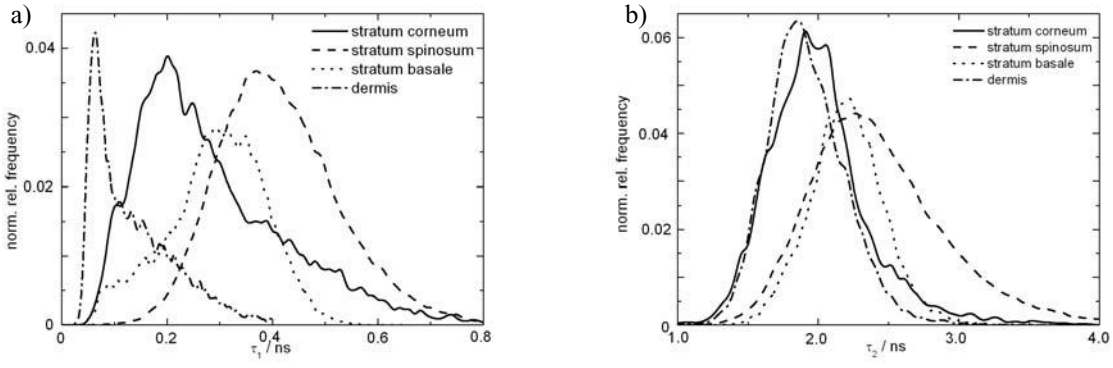

Figure 7: Fluorescence lifetime distribution of a) the fast component and b) for the slow component of the different human skin layers.

The peaks of the fast components $_1$ of the different skin layers vary between 0.2 and 0.4ns. Only the strong peak of the dermis distribution shows a lifetime in the region of the IRF. This peak is due to the SHG emanating from collagenous material in the dermis. The long shoulder is due to the autofluorescence from collagen. However, a clear distinction between the different dermal layers can not be seen in the different distributions. Layers with living cells (stratum spinosum and stratum basale) exhibited a longer fluorescence characteristic.
The slow components are shown in Fig. 6 b). Their peaks vary between 1.8 and 2.5 ns. Both the stratum spinosum and the stratum basale have a slower decay characteristic than the keratinous stratum corneum or the fluorescence of the collagen-rich dermis. This can be attributed to the living cells in the former two skin layers.

3.2 FLIM of human hairs

In Fig. 7 a typical image of the surface of a black hair (cuticle, Fig.7a), a black hair in the depth of z=20µm (cortex, Fig. 7b) and a blond hair in z=20µm are shown (Fig.7 a). the typical appearance of the cuticle can be observed. For both black and blond hairs, the surface structure was found to be the same. However, if the deeper areas of the cortex were examined, black and blond hairs show distinct fluorescence behaviour. In blond hairs the fibrous structure of the cortex was seen over the whole area of the hair. In the case of black hairs the outer areas appeared to be brighter and the fibrous structure could not be seen any more.

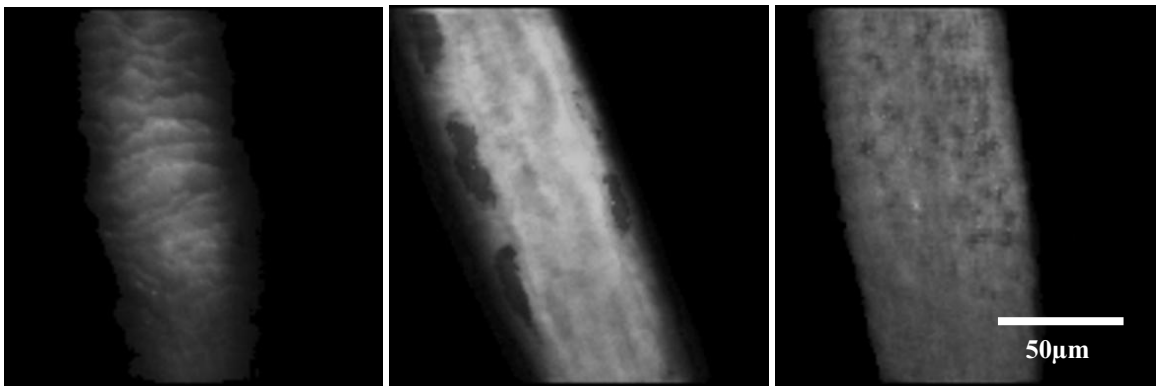

Figure 8: a) Cuticle of a black human hair. b) FLIM image of a black human hair and c) FLIM image of a blond human hair in a depth of 20µm.

In a false colour image displaying the slow fluorescence decay component, these outer areas have a clearly longer decay time than the inner areas. A darker colour corresponds to a longer lifetime. In blond hairs the distribution of the decay times is more homogenous spread over the whole hair. Since eumelanin is responsible for the black coloration and the melanin granules are mainly in the outer areas, this behaviour of the fluorescent lifetime distribution can be attributed to eumelanin. The distributions of the two lifetime decay components $_1$ and $_2$ are shown (Fig. 9a).

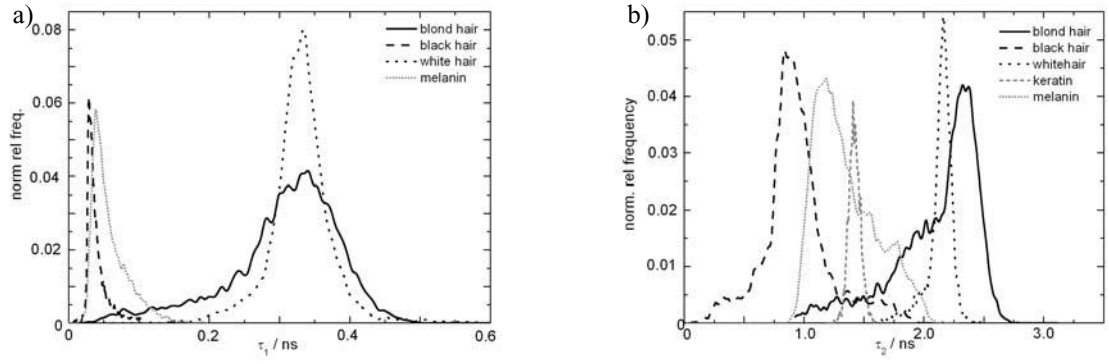

Figure 9: Fluorescence lifetime distribution of a) the fast component of the different human hair types and artificial components and b) for the slow component.

The fast decay components show a clear distinction between the different hair colorations. Hair rich with eumelanin shows a short and narrow distribution with a peak at 0.03ns with FWHM of 0.03ns. This corresponds to the lifetime decay characteristics found for DOPA melanin with peak at 0.04ns and FWHM 0.03ns. For hairs containing no eumelanin, the lifetime distribution of $_1$ appears to be broader with an elongated shoulder with a peak at 0.34ns a with FWHM 0.12. White hairs do not posses melanin. In Fig. 8a) the peaks of the distributions of white and blond hairs coincide, but the FWHM of white hairs with 0.06ns is smaller. Therefore, a clear distinction between pheomelanin and the absence of melanin can not be made.
The slow components show a clear distinction between hair types according to distribution data as well. The typical lifetime distributions of blond and red hairs have a peak at 2.3ns with FWHM 0.3ns. In contrast, black hairs have a peak at 0.8ns with FWHM 1.3ns. Compared to the lifetime distributions in human skin, the peaks are very sharp and the FWHM. It is evident, that the two hair types can be distinguished easily. The slow DOPA-melanin lifetime shows a peak at1.2ns wirh FWHM 0.4ns. Keratin has a peak at about 1.4ns with FWHM 0.1ns. From Fig. 8b) it becomes evident that eumelanin is responsible for the faster decay times of $_2$, whereas mainly pheomelanin is responsible for slower decay times of t $_2$ of about 2.5ns. The role of keratin components in hairs is not that clear. Artificial keratin seems to have a very narrow distribution only slightly slower than that of eumelanin. On the contrary, the lifetime distribution of the human stratum corneum is different from artificial pure keratin. This is interesting, since the stratum corneum mainly consists of keratin. It is broader distributed with a peak at about 2ns. This leads to the assumption, that keratin is indirectly visible in the fluorescence lifetime distribution of $_2$ of skin and hairs. However, he main characteristic in hairs is due to the different melanin types.

4. CONCLUSIONS

Human skin and hair were measured with an ultrafast fluorescence lifetime detection system with an IRF of 24ps. The resulting lifetime decay curves were fitted with a bi-exponential model showing a rather short fast component. The distributions of the different lifetimes were examined to analyze which fluorophores give rise to the fluorescence signal.
From earlier measurements of human skin it was not clear, if the fast decay component of is due to scattering, SHG, Raman or other effects. The measurements in this work show that this fast component is not in the range of the IRF of the imaging system and therefore not due to such an immediate effect in the tissue. The nature of the luminescence of human tissue still have to be further investigated.
Comparison of the lifetime decay distributions of the examined tissue with pure fluorophores either extracted from human skin or fabricated artificially help to identify the endogenous fluorophores. Their distributions are broader compared to the pure fluorophores. This is due to a mixing of different fluorophores and different microenvironments. This work shows that FLIM of human tissue and tissue appendages *in vivo* is possible for fast and painless analysis of chemical components and states.

5. REFERENCES

1. B. R. Masters, P. T. So, E. Gratton, ”Multiphoton excitation fluorescence microscopy and spectroscopy of in vivo human skin”, Biophys. J. 72: 2405-2412 (1997).
2. B. R. Masters, P. T. So, E. Gratton, ” Multiphoton excitation microscopy of in vivo human skin: Functional and morphological optical biopsy based on three-dimensional imaging, lifetime measurements and fluoresence spectroscopy”, Ann. N.Y. Acad. Sci. 838:5867 (1998).
3. R. F. Hendriks, G. W. Lucassen, ”Two photon fluorescence microscopy of in vivo human skin”, Proc. SPIE 4164: 116-121 (2000).
4. K. König, I. Riemann, ”High-resolution multiphoton tomography of human skin with subcellular spatial resolution and picosecond time resolution”, J. Biomed. Opt. 8(3): 432-439 (2003).
5. T. Richter, C. Peuckert, M. Sattler, et al., ”Dead but highly dynamic - the stratum corneum is divided into

three hydration zones", Skin Pharmacol. Physiol. 17: 246-257 (2004).
6. P. J. Caspers, G. W. Lucassen, E. A. Carter, H. A. Bruining, G. J. Puppels, "In vivo confocal Raman Microspectroscopy of the skin: noninvasive determination of molecular concentration profiles", J. Invest. Derm. 116(3): 434-442 (2001).
7. 7. M. Corsi, G. Cristoforetti, M. Hidalgo, et al., "Application of laser-induced breakdown spectroscopy technique to hair tissue mineral analysis", Appl. Optics 42(30): 6133-6137 (2003).
8. P. Hallégot, R. Peteranderl, C. Lechene, "In-situ imaging mass spectrometry analysis of melanin granules in the human hair shaft", J. Invest. Dermat. 122: 381-386 (2004).
9. K. Jimbow, O. Ishida, S. Ito, Y. Hori, C. J. Witkop, R. A. King, "Combined chemical and Electron Microscopic studies of phemelanosomes in human red hair" J. Invest. Dermat. 81(6): 506-511 (1983).
10. H. Zahn, "Feinbau und Chemie des Haares", Parfümerie und Kosmetik 65(9), 507-594 (1984).
11. D. Van Neste (ed.) Hair Science and technology, Skinterface: Tournai-Belgium, (2003).
12. V. Ulrich, P. Fischer, I. Riemann, K. König, „Compact Multiphoton / Single Photon laser scanning microscope for spectral imaging and Fluorescence lifetime imaging", Scanning 26:217-225 (2004)